Semiclassical model of stimulated Raman scattering in photonic crystals

Lucia Florescu* and Xiang Zhang
5130 Etcheverry Hall, NSF Nano-scale Science and Engineering Center, University of California, Berkeley, California 94720-1740, USA
(Received 29 March 2005; published 13 July 2005)

We study the stimulated Raman scattering (SRS) of light from an atomic system embedded in a photonic crystal and coherently pumped by a laser field. In our study, the electromagnetic field is treated classically and the atomic system is described quantum mechanically. Considering a decomposition of the pump and Stokes fields into the Bloch modes of the photonic crystals and using a multiscale analysis, we derive the Maxwell-Bloch equations for SRS in photonic crystals. These equations contain effective parameters that characterize the SRS gain, the nonlinear atomic response to the electromagnetic field, and the group velocity and that can be calculated in terms of the Bloch modes of the unperturbed photonic crystal. We show that if the pump laser frequency is tuned near a photonic band edge and the atomic system is carefully chosen such that the Stokes mode matches another photonic band edge, low-threshold, enhanced Raman amplification is possible. Possible physical realizations of SRS in photonic crystals are also discussed.

DOI: 10.1103/PhysRevE.72.016611 PACS number(s): 42.70.Qs, 42.65.Dr

I. INTRODUCTION

Photonic crystals are periodic dielectric materials in which light propagation can be prohibited over a certain range of frequencies, known as the photonic band gap. The possibility of achieving photon localization [1] and photonic band gaps [2,3] in photonic crystals has motivated new research directions, and novel applications meant to improve the performances of optoelectronic and microwave devices have been considered. These applications include low threshold, high efficiency microlasers [4–8], ultrafast all-optical switches [9,10], or all-optical microtransistors [11].

A promising application of the photonic crystals is in the field of Raman spectroscopy. One of the most efficient Raman spectroscopic techniques is based on the strongly surface-enhanced Raman scattering effect (SERS) [12] achieved in metallodielectric structures. In this case, the enhancement of the Raman scattering rate and, implicitly, of the Raman signal, is facilitated by the strong local enhancement of the electromagnetic field. Similarly, the possibility to engineer the photonic density of states and the photonic mode structure in a desired fashion in photonic crystals is expected to strongly modify the Raman scattering of light from active elements embedded in these structures. For instance, near a photonic band edge, spontaneous Raman scattering is expected [13,14] to be strongly enhanced and to possess unusual spectral properties, as a result of the enhancement and rapid variation as a function of frequency of the photonic density of states. The Raman signal enhancement could be of relevance in molecular spectroscopy, and purely dielectric photonic crystals may constitute a better alternative to the conventional metallic systems, which present high losses at optical frequencies.

The process of Raman scattering in photonic crystals has attracted increasing interest recently. Previous theoretical studies have addressed the problem of spontaneous Raman scattering [13,14], or considered the stimulated Raman scattering (SRS) in one-dimensional photonic crystals [15]. Specifically, a quantum theory of resonance Raman scattering of light from an atomic system embedded in a photonic band-gap material has been developed [13]. This theory enables the investigation of the intensity of the spontaneous Raman scattering signal as well as its spectral properties. Moreover, an analysis of the effect of the photonic density of states on spontaneous Raman scattering rate in photonic crystals has been presented in Ref. [14].

The problem of SRS in photonic crystals has been previously addressed for the case of one-dimensional photonic crystals. In this case, numerical simulations of SRS of a femtosecond pulse [15,16] have shown that the SRS conversion is more efficient when the Stokes frequency lies on the photonic band gap edge. In this paper we address the process of SRS in one- and two-dimensional photonic crystals. We derive the generalized semiclassical Maxwell-Bloch equations for SRS in photonic crystals and further employ this formalism to investigate the SRS characteristics. Our effective model has the advantage of allowing for a detailed investigation of the SRS problem without having to numerically solve the nonlinear problem. Central to the discussion presented here are the photonic band structure of the underlying photonic crystal and the redistribution and enhancement of the field energy in the associated Bloch modes. We demonstrate that a low-threshold, enhanced SRS process is possible if both the pump field frequency and Stokes transition frequency are near two photonic band edges, as a result of strong enhancement of both pump and Stokes fields, and low group velocities at these frequencies [16].

In Sec. II we present the general semiclassical equations for SRS and derive the effective Maxwell-Bloch equations for SRS in photonic crystals. In Sec. III we investigate the effect of the photonic crystals on the SRS threshold and Raman signal and present a possible practical realization of SRS in photonic crystals. In Sec. IV we discuss the results and possible generalizations of the model developed here.

*Present address: NASA Jet Propulsion Laboratory, California Institute of Technology, MS 126-347, 4800 Oak Grove Drive, Pasadena, CA 91109, USA.

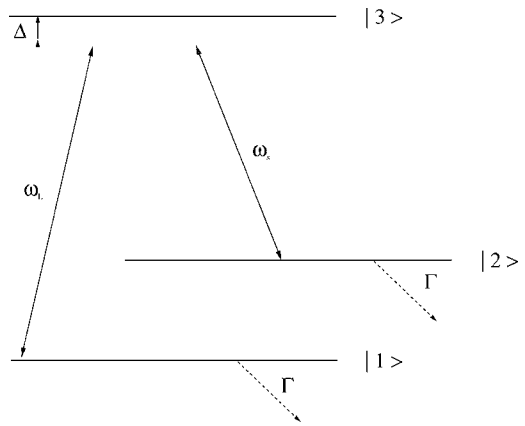

FIG. 1. Three-level system in Λ configuration coupled by a pump laser field of frequency ω_L and a Stokes laser field of frequency ω_s. Continuous arrows denote the dipole allowed transitions, and the dashed arrows denote the decay processes. Δ is the detuning between the pump laser frequency and the atomic transition frequency between levels $|3\rangle$ and $|1\rangle$, and Γ is the relaxation rate.

II. SEMICLASSICAL EQUATIONS FOR STIMULATED RAMAN SCATTERING

In this section we review the general equations describing the process of stimulated Raman scattering. Then, using a multiple scale analysis, we derive the generalized semiclassical Maxwell-Bloch equations for stimulated Raman scattering in photonic crystals.

A. Model

We consider a periodic dielectric medium doped with resonant three-level atoms in Λ configuration (presented in Fig. 1) acting as a Raman medium. Let $|1\rangle$ denote the atomic ground level and let $|2\rangle$ and $|3\rangle$ denote the two excited levels. A pump laser field with frequency ω_L, driving the transition between levels $|1\rangle$ and $|3\rangle$, propagates through the medium and is scattered by the resonant atoms to produce photons at the Stokes frequency $\omega_S=\omega_L-\omega_{21}$, where $\hbar\omega_{21}$ is the energy of the final state $|2\rangle$ above the ground state $|1\rangle$. There are no direct allowed dipolar transitions between levels $|1\rangle$ and $|2\rangle$. Further, this three-level model can be exactly reduced to a two-level model by the use of an effective Raman theory [17,18], in which level $|3\rangle$ is adiabatically eliminated. In this case, the two atomic levels $|1\rangle$ and $|2\rangle$ are coupled through an effective coupling constant λ (depending on the dipole-coupling constants between levels $|1\rangle$ and $|3\rangle$, and $|2\rangle$ and $|3\rangle$, respectively), and the effective two-level Raman interaction Hamiltonian describing the interaction between the pump and Stokes radiation modes and the atomic system has the usual Jaynes-Cummings form [19], in which the single-mode field operators are replaced by products of an annihilation operator of one mode and the creation operator of the other: $H_i=\hbar\lambda(a_s^\dagger a_L\sigma_{21}+a_L^\dagger a_s\sigma_{12})$. Here, $a_s^\dagger$ and a_s represent the Stokes field creation and annihilation operators, $a_L^\dagger$ and a_L are the laser field creation and annihilation operators, and $\sigma_{ij}=|i\rangle\langle j|$ $(i,j=1,2,i\neq j)$ are the atomic transition operators from level $|j\rangle$ to level $|i\rangle$. Due to the simplicity of this effective two-level model, leading to a reduced system of equations describing the dynamics of the system, we will employ it to the derivation of an effective semiclassical model of SRS in photonic crystals.

In the present study, we assume that the laser fields are strong enough such that they can be treated classically. In this case, the coupled atom-field system is described by the semiclassical Maxwell-Bloch equations. Also, we assume that in a one-dimensional (1D) photonic crystal electromagnetic waves propagate perpendicular to the dielectric layers of the photonic crystals, whereas in the two-dimensional (2D) case we assume that the electromagnetic wave propagates in the plane of periodicity with the electric field polarized perpendicular to this plane (TM modes). Thus the electromagnetic field propagation through the nonlinear medium is described by a scalar wave equation. The wave equation for the Stokes field $E_s(\mathbf{x},t)$ reads [17]:

$$\nabla^2 E_s(\mathbf{x},t)-\frac{\epsilon(\mathbf{x})}{c^2}\frac{\partial^2 E_s(\mathbf{x},t)}{\partial t^2}=\kappa\frac{4\pi}{c^2}\frac{\partial^2}{\partial t^2}P_{21}(\mathbf{x},t)E_L(\mathbf{x},t), \tag{2.1}$$

where $\epsilon(\mathbf{x})$ is the periodic dielectric function and $E_L(\mathbf{x},t)$ is the pump laser field. The collective nonlinear polarization density of the medium due to the presence of resonant three-level atoms, $P_{12}(\mathbf{x},t)$, is associated with the coherence between levels $|1\rangle$ and $|2\rangle$ [17] and will be defined below. The atom-field coupling constant κ is given by [17] $\kappa\approx d_{13}d_{23}/\hbar^2\Delta$, where d_{13} and d_{23} are the dipole moments of the allowed atomic transitions $|3\rangle\rightarrow|1\rangle$ and $|3\rangle\rightarrow|2\rangle$, respectively, and $\Delta=\omega_{31}-\omega_L$ is the detuning between the atomic transition frequency and the laser pump frequency (ω_{31} is the frequency separation between levels $|3\rangle$ and $|1\rangle$). Here, we neglect the depletion of the laser fields due to the absorption by the nonresonant atoms or other material losses. The pump laser field $E_L(\mathbf{x},t)$ obeys a wave equation similar equation to Eq. (2.1), in which $P_{21}(\mathbf{x},t)$ is replaced by $P_{21}^*(\mathbf{x},t)$.

The collective polarization $P_{21}(\mathbf{x},t)$ is defined in terms of single-atom polarizations, $P_a(t)$, as

$$P_{21}(\mathbf{x},t)=\sum_a \delta(\mathbf{x}-\mathbf{x}_a)P_a(t)=n(\mathbf{x})P(\mathbf{x},t). \tag{2.2}$$

Here, the summation is over the Raman atoms, embedded in the photonic crystal at position $\mathbf{x}_a$, $P(\mathbf{x},t)$ denotes the atomic polarization density at position $\mathbf{x}$, and the weight function $n(\mathbf{x})$ characterizes the distribution of Raman-active material within the photonic crystal [$n(\mathbf{x})=1$ for a uniform distribution of the Raman atoms].

The atomic Bloch equations describing the response of the atomic medium to the electromagnetic field follow from the Heisenberg equation of motion for the atomic density operator, $\rho=\Sigma_{i,j}\rho_{ij}|i\rangle\langle j|$, which has the form $i\hbar\partial\rho/\partial t=[H,\rho]+(\partial\rho/\partial t)_d$. Here, H is the Hamiltonian of the system, and $(\partial\rho/\partial t)_d$ describes the damping processes, such as radiative and nonradiative spontaneous emission and other dephasing effects. Using the effective two-level Raman model for the three-level atom in Λ configuration, we arrive at the follow-

ing atomic Bloch equations for the atomic polarization $P_a(t) \equiv \rho_{21}$ and atomic population inversion $\Delta N_a \equiv \rho_{22} - \rho_{11}$ between the final state $|2\rangle$ and the ground state $|1\rangle$ [17]:

$$\frac{dP_a(t)}{dt} = i\omega_{21}P_a(t) - \gamma P_a(t) - i\kappa E_s(\mathbf{x}_a,t)E_L^*(\mathbf{x}_a,t)\Delta N_a(t), \tag{2.3}$$

$$\frac{d\Delta N_a(t)}{dt} = -\Gamma(\Delta N_a(t)+1) + 2i\kappa[E_s(\mathbf{x}_a,t)E_L^*(\mathbf{x}_a,t)P_a^*(t) - E_s^*(\mathbf{x}_a,t)E_L(\mathbf{x}_a,t)P_a(t)]. \tag{2.4}$$

Here, the damping effects have been included phenomenologically through the relaxation rates γ (describing the collision dephasing of the dipole moment) and Γ (describing the relaxation of the atomic levels). The second term on the right-hand side of Eq. (2.4) describes the rate of adding atoms into the interaction region.

B. Semiclassical Maxwell-Bloch equations for SRS in photonic crystals

In what follows, we will derive the semiclassical equations for SRS in photonic crystals by performing a multiscale analysis [20,21] of the Maxwell-Bloch Eqs. (2.1)–(2.4). This analysis is analogous to the slowly varying envelope approximation employed in the case of conventional stimulated Raman scattering [17], and has been successfully applied to investigate various nonlinear phenomena in photonic crystals [22,7].

We first note that the nonlinear term on the right-hand side of the wave Eq. (2.1) can be rewritten as $(\Omega_L/\Delta)d_{32}P(\mathbf{x},t)$, where $\Omega_L \equiv d_{31}E_L/\hbar$ is the Rabi frequency of the pump field (usually of the same order of magnitude as Δ). For usual densities of resonant atoms and in the linear regime, $d_{32}P(\mathbf{x},t) \simeq \chi E(\mathbf{x},t)$, the optical susceptibility χ is of the order of 10^{-8} [23]. As a result, the nonlinear term in wave Eq. (2.1) has a much smaller contribution than the remaining terms describing the free evolution of the electromagnetic field. This fact is taken into account in our formalism by introducing a small perturbation parameter $\mu \approx \chi \approx 10^{-8}$ into the wave Eq. (2.1), and rewriting it as

$$\nabla^2 E_s(\mathbf{x},t) - \frac{\epsilon(\mathbf{x})}{c^2}\frac{\partial^2 E_s(\mathbf{x},t)}{\partial t^2} = \mu\kappa\frac{4\pi}{c^2}n(\mathbf{x})\frac{\partial^2}{\partial t^2}P(\mathbf{x},t)E_L(\mathbf{x},t). \tag{2.5}$$

Here we have also used the expression (2.2) for the nonlinear collective atomic polarization $P_{21}(\mathbf{x},t)$ entering the wave Eq. (2.1).

On the other hand, the atomic relaxation rates Γ and γ (corresponding to nanoseconds time scale) are much smaller than the optical frequency by a factor of 10^7 or more ($\approx 1/\mu$). Also, the driving terms (the terms containing the electric fields) in the Bloch Eqs. (2.3) and (2.4) can be rewritten as $(\Omega_L\Omega_s/\Delta)\Delta N_a$ and $(\Omega_L\Omega_s/\Delta)P_a$, respectively, where the Rabi frequencies of the Stokes and pump fields, $\Omega_s \equiv d_{23}E_s/\hbar$ and $\Omega_L \equiv d_{13}E_L/\hbar$, are usually much smaller than the optical frequency (by more than six orders of magnitude, for a system operation below the saturation regime [7]). As a result, the terms describing the relaxation processes as well as the driving terms have much smaller contributions than the remaining terms in the Bloch Eqs. (2.3) and (2.4),

$$\gamma P_a, \frac{\Omega_L\Omega_s}{\Delta}\Delta N \ll \omega_{21}P_a \tag{2.6}$$

and

$$\Gamma\Delta N, \frac{\Omega_L\Omega_s}{\Delta}P_a \ll \frac{d\Delta N_a}{dt}. \tag{2.7}$$

Consequently, we introduce the perturbation parameter μ also into Eqs. (2.3) and (2.4) and rewrite them for the atomic polarization and population inversion densities, $P(\mathbf{x},t)$ and $N(\mathbf{x},t)$, as

$$\frac{dP(\mathbf{x},t)}{dt} = i\omega_{21}P(\mathbf{x},t) - \mu\gamma P(\mathbf{x},t) - i\mu\kappa E_s(\mathbf{x},t)E_L^*(\mathbf{x},t)\Delta N_a(\mathbf{x},t), \tag{2.8}$$

$$\frac{d\Delta N(\mathbf{x},t)}{dt} = \mu\{-\Gamma(\Delta N(\mathbf{x},t)+\mathcal{N}) + 2i\kappa[E_s(\mathbf{x},t)E_L^*(\mathbf{x},t)P^*(\mathbf{x},t) - E_s^*(\mathbf{x},t)E_L(\mathbf{x},t)P(\mathbf{x},t)]\}. \tag{2.9}$$

These equations have been obtained from Eqs. (2.3) and (2.4) after multiplying them by $\delta(\mathbf{x}-\mathbf{x}_a)$ and summing over the atoms and are valid only for the positions $\mathbf{x}$ within the sample where there are atoms. In Eq. (2.9), $\mathcal{N}$ is the number of Raman atoms in the system.

The multiple-scale analysis [20] is based on the separation of the fast variations from slow variations in space and time in the electromagnetic field and atomic variables. To this end, the space and time variables, $\mathbf{x}$ and t, are replaced by a set of independent variables, $\mathbf{x}_n \equiv \mu^n\mathbf{x}$ and $t_n \equiv \mu^n t$, respectively, where the fastest spatial scale, $\mathbf{x}_0$, corresponds to the wavelength of electromagnetic waves propagating in the photonic crystal, and the fastest temporal scale, t_0, corresponds the optical period $2\pi/\omega$. The spatial and time derivatives can be calculated in terms of these variables as

$$\frac{\partial}{\partial q} = \frac{\partial}{\partial q_0} + \mu\frac{\partial}{\partial q_1} + \mu^2\frac{\partial}{\partial q_2} + \cdots, \tag{2.10}$$

where $q = \mathbf{x}, t$. Also, we consider perturbational expansions of the electromagnetic fields $E_L(\mathbf{x},t)$ and $E_s(\mathbf{x},t)$ and atomic variables $P(\mathbf{x},t)$ and $\Delta N(\mathbf{x},t)$ of the form

$$f(\mathbf{x},t) = f^{(0)} + \mu f^{(1)} + \mu^2 f^{(2)} + \cdots. \tag{2.11}$$

In our study we consider that while both the electromagnetic fields $E^{(n)} = E^{(n)}(\mathbf{x}_0,\mathbf{x}_1,\ldots;t_0,t_1,\ldots)$ and atomic polarization $P^{(n)} = P^{(n)}(\mathbf{x}_0,\mathbf{x}_1,\ldots;t_0,t_1,\ldots)$ vary on all spatial and temporal scales, the atomic inversion ΔN does not vary on the fastest temporal scale t_0, $\Delta N^{(n)} = \Delta N^{(n)}(\mathbf{x}_0,\mathbf{x}_1,\ldots;t_1,t_2,\ldots)$, as the atomic transitions occur on a much smaller time scale

(of the order of nanoseconds), compared with the optical time scale [23]. Also, we assume that the periodic dielectric function $\epsilon(\mathbf{x})=\epsilon(\mathbf{x}_0)$ and the atomic distribution function $n(\mathbf{x})=n(\mathbf{x}_0)$ vary only on the smallest length scale $\mathbf{x}_0$. Introducing into the Eqs. (2.5), (2.8), and (2.9) the expansions of the form (2.11) of various atomic and field functions, together with the expansions of the time and space derivatives calculated according to Eq. (2.10), we generate a set of equations, corresponding to various powers of the expansion parameter μ. On the fastest scale (zeroth order in μ), we obtain:

$$\left[\frac{\partial^2}{\partial \mathbf{x}_0^2}-\frac{\epsilon(\mathbf{x})}{c^2}\frac{\partial^2}{\partial t_0^2}\right]E^{(0)}=0, \tag{2.12}$$

$$\frac{\partial P^{(0)}}{\partial t_0}=i\omega_{21}P^{(0)}, \tag{2.13}$$

while on the slow scale (first order in μ), we have

$$\left[-c^2\frac{\partial^2}{\partial \mathbf{x}_0^2}+\epsilon(\mathbf{x}_0)\frac{\partial^2}{\partial t_0^2}\right]E^{(1)}=\left[2c^2\frac{\partial}{\partial \mathbf{x}_0}\frac{\partial}{\partial \mathbf{x}_1}-2\epsilon(\mathbf{x}_0)\frac{\partial}{\partial t_0}\frac{\partial}{\partial t_1}\right]E^{(0)}+4\pi\kappa n(\mathbf{x}_0)\frac{\partial^2}{\partial t_0^2}P^{(0)}E_L^{(0)}, \tag{2.14}$$

$$\left[\frac{\partial}{\partial t_0}-i\omega_{21}\right]P^{(1)}+\frac{\partial}{\partial t_1}P^{(0)}=-\gamma P^{(0)}-i\kappa E_s^{(0)}E_L^{*(0)}\Delta N^{(0)}, \tag{2.15}$$

$$\frac{d\Delta N^{(0)}}{dt_1}=-\Gamma[\Delta N^{(0)}+\mathcal{N}]+2i\kappa[E_s^{(0)}E_L^{*(0)}P^{*(0)}-E_s^{*(0)}E_L^{(0)}P^{(0)}]. \tag{2.16}$$

Next, we consider a decomposition of $E^{(n)}$ and $P^{(n)}$ into the eigenfunctions $\{\Phi_m(\mathbf{x}_0)\}$ of the photonic crystal, which are the solutions of the homogeneous wave equation

$$\left[\frac{\partial^2}{\partial \mathbf{x}_0^2}+\frac{\omega_m^2}{c^2}\epsilon(\mathbf{x}_0)\right]\Phi_m(\mathbf{x}_0)=0, \tag{2.17}$$

where ω_m are the associated eigenfrequencies. $\{\Phi_m(\mathbf{x}_0)\}$ satisfy the orthogonality relations

$$\int_{\text{cell}}\Phi_m^*(\mathbf{x}_0)\epsilon(\mathbf{x}_0)\Phi_{m'}(\mathbf{x}_0)d\mathbf{x}_0=\delta_{m,m'}, \tag{2.18}$$

where the integral is over the unit cell of the photonic crystal. In the present study we assume that only one mode in the expansion of the electromagnetic zeroth-order field contributions is dominant,

$$E_s^{(0)}(\mathbf{x}_0,\mathbf{x}_1,\ldots;t_0,t_1,\ldots)=\mathcal{E}_s(\mathbf{x}_1,\mathbf{x}_2,\ldots;t_1,t_2,\ldots)\times\Phi_m(\mathbf{x}_0)e^{-i\omega_m t_0}, \tag{2.19}$$

$$E_L^{(0)}(\mathbf{x}_0,\mathbf{x}_1,\ldots;t_0,t_1,\ldots)=\mathcal{E}_L(\mathbf{x}_1,\mathbf{x}_2,\ldots;t_1,t_2,\ldots)\times\Phi_n(\mathbf{x}_0)e^{-i\omega_n t_0}, \tag{2.20}$$

where the coefficients $\mathcal{E}_{s,L}$ play the role of the slowly varying envelope functions in the conventional case. Here, we consider that the modes Φ_m and Φ_n are distinct, $m\neq n$, and will call these modes the Stokes mode and the pump mode, respectively. On the other hand, Eq. (2.8) suggests a decomposition of the atomic polarization of the form

$$P^{(0)}(\mathbf{x}_0,\mathbf{x}_1,\ldots;t_0,t_1,\ldots)=\mathcal{P}(\mathbf{x}_1,\mathbf{x}_2,\ldots;t_1,t_2,\ldots)\times\Phi_m(\mathbf{x}_0)\Phi_n^*(\mathbf{x}_0)e^{-i(\omega_m-\omega_n)t_0}. \tag{2.21}$$

For the first-order corrections $E^{(1)}$ and $P^{(1)}$ we assume that all the other eigenmodes of the photonic crystal contribute, except for the Stokes and pump modes:

$$E_s^{(1)}(\mathbf{x}_0,\mathbf{x}_1,\ldots;t_0,t_1,\ldots)=\sum_{m'\neq m,n}e_{s,m'}(\mathbf{x}_1,\mathbf{x}_2,\ldots;t_1,t_2,\ldots)\times\Phi_{m'}(\mathbf{x}_0)e^{-i\omega_{m'}t_0}, \tag{2.22}$$

$$E_L^{(1)}(\mathbf{x}_0,\mathbf{x}_1,\ldots;t_0,t_1,\ldots)=\sum_{n'\neq n,m}e_{L,n'}(\mathbf{x}_1,\mathbf{x}_2,\ldots;t_1,t_2,\ldots)\times\Phi_{n'}(\mathbf{x}_0)e^{-i\omega_{n'}t_0}, \tag{2.23}$$

$$P^{(1)}(\mathbf{x}_0,\mathbf{x}_1,\ldots;t_0,t_1,\ldots)=\sum_{m',n'\neq m,n}p(\mathbf{x}_1,\mathbf{x}_2,\ldots;t_1,t_2,\ldots)\times\Phi_{m'}(\mathbf{x}_0)\times\Phi_{n'}^*(\mathbf{x}_0)e^{-i(\omega_{m'}-\omega_{n'})t_0}. \tag{2.24}$$

We further insert the expansions (2.19)–(2.24) into the Eqs. (2.12)–(2.16). Eqs. (2.19) and (2.20) together with Eq. (2.12) lead to the wave Eq. (2.17). On the other hand, Eqs. (2.21) and (2.13) lead to the frequency resonance condition

$$\omega_n-\omega_m=\omega_{21}. \tag{2.25}$$

This is exactly the frequency down-conversion condition for the Raman Stokes effect.

In order to obtain the equations of motion for the envelope functions $\mathcal{E}_s$ and $\mathcal{P}$, we insert expansions (2.19)–(2.24) into the first-order Eqs. (2.14)–(2.16), use the frequency resonance condition (2.25), project the resulting system of equations onto the subspace spanned by the Stokes field dominant mode Φ_m, use the orthogonality condition (2.18) and that Eqs. (2.15) and (2.16) are only valid at the position where there is a nonzero atom distribution. We obtain:

$$\mathbf{v}_m\cdot\boldsymbol{\nabla}\,\mathcal{E}_s(\mathbf{x},t)+\frac{\partial\mathcal{E}_s(\mathbf{x},t)}{\partial t}=-\gamma_m\mathcal{E}_s(\mathbf{x},t)+2\pi i\kappa\omega_m\alpha_{mn}\mathcal{P}(\mathbf{x},t)\mathcal{E}_L(\mathbf{x},t), \tag{2.26}$$

$$\frac{\partial\mathcal{P}(\mathbf{x},t)}{\partial t}=-\gamma\mathcal{P}(\mathbf{x},t)-i\kappa\mathcal{E}_s(\mathbf{x},t)\mathcal{E}_L^*(\mathbf{x},t)\widetilde{\Delta N}(\mathbf{x},t), \tag{2.27}$$

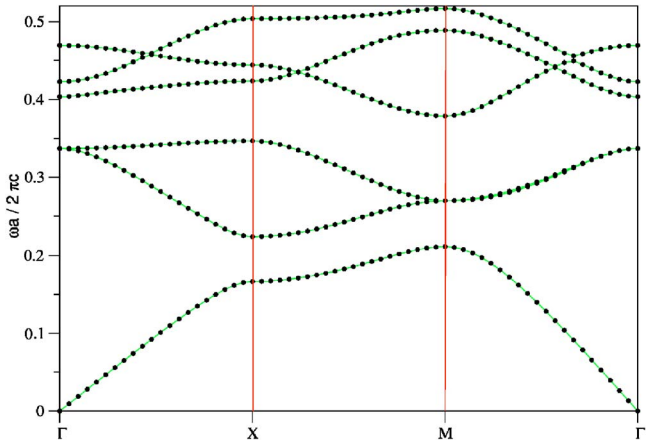

FIG. 2. (Color online) The TM photonic band structure of a 2D photonic crystal consisting of a square array of dielectric (ϵ=12) cylinders with radius r=0.4a (where a is the lattice constant) in air (ϵ=1).

$$\frac{\partial\widetilde{\Delta N}(\mathbf{x},t)}{\partial t} = -\Gamma(\widetilde{\Delta N}(\mathbf{x},t) + \mathcal{N}) + 2i\kappa\beta_{mn}[\mathcal{E}_s(\mathbf{x},t)\mathcal{E}_L^*(\mathbf{x},t)\mathcal{P}^*(\mathbf{x},t) - \mathcal{P}(\mathbf{x},t)\mathcal{E}_s^*(\mathbf{x},t)\mathcal{E}_L(\mathbf{x},t)]. \quad (2.28)$$

Here, we have truncated the multiscale hierarchy on the scale of $\mathbf{x}_1$ and t_1, and used the notation $\mathbf{x}\equiv\mathbf{x}_1$ and $t\equiv t_1$. Eqs. (2.26)–(2.28) represent the effective semiclassical equations for stimulated Raman scattering in photonic crystals. They describe the coupling between the atomic medium and electromagnetic fields in photonic crystals, and from their solutions the spatial and temporal characteristics of the Stokes field can be obtained. We note that these equations are similar to those for stimulated Raman scattering in free space [17]. Additionally, they contain effective parameters related to the linear properties of the underlying photonic crystal, $\mathbf{v}_m$, α_{mn}, and β_{mn}, with well-defined physical meaning. $\mathbf{v}_m$ in Eq. (2.26) for the field envelope function represents the group velocity of a pulse with carrier wave $\Phi_m(\mathbf{x}_0)$ [21,24,25] and is defined by

$$\mathbf{v}_m = \frac{c^2}{\omega_m}\int_{\text{cell}} \Phi_m^*(\mathbf{x}_0)\left(-i\frac{d}{d\mathbf{x}_0}\right)\Phi_m(\mathbf{x}_0)d\mathbf{x}_0. \quad (2.29)$$

The effective Raman gain parameter α_{mn} and nonlinear coupling parameter β_{mn} in Eqs. (2.26) and (2.28) are defined by

$$\alpha_{mn} = \int_{\text{cell}} |\Phi_m(\mathbf{x}_0)|^2|\Phi_n(\mathbf{x}_0)|^2 n(\mathbf{x}_0)d\mathbf{x}_0 \quad (2.30)$$

and

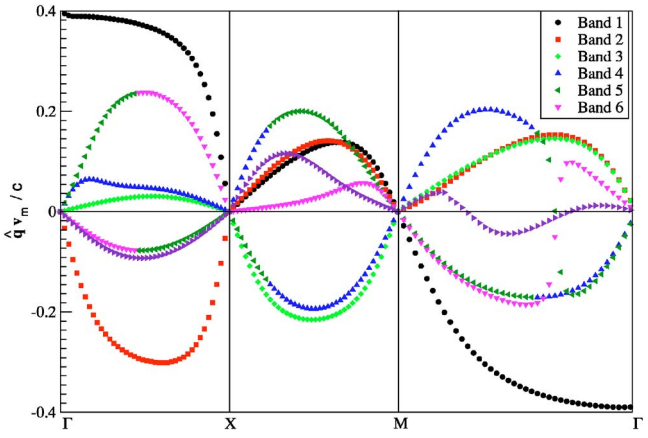

FIG. 3. (Color online) The group velocity for the lowest bands of the TM photonic band structure of the 2D photonic crystal presented in Fig. 2.

$$\beta_{mn} = \frac{\int_{\text{cell}} |\Phi_m(\mathbf{x}_0)|^4|\Phi_n(\mathbf{x}_0)|^4 n(\mathbf{x}_0)d\mathbf{x}_0}{\int_{\text{cell}} |\Phi_m(\mathbf{x}_0)|^2|\Phi_n(\mathbf{x}_0)|^2 n(\mathbf{x}_0)d\mathbf{x}_0}, \quad (2.31)$$

respectively. We have phenomenologically introduced into the field-propagation Eq. (2.26) a cavity-loss rate, γ_m, related to the finite-size effects in photonic crystals. It has been suggested [26] that a finite photonic crystal can be regarded as a Fabry-Perot resonator, whose cavity-leakage rate γ_m depends on the group velocity.

The effective atomic population inversion, $\widetilde{\Delta N}(\mathbf{x},t)$, is defined by

$$\widetilde{\Delta N}(\mathbf{x},t) \equiv \frac{\int_{\text{cell}} \Delta N(\mathbf{x}_0,\mathbf{x}_1;t_1)|\Phi_m(\mathbf{x}_0)|^2|\Phi_n(\mathbf{x}_0)|^2 n(\mathbf{x}_0)d\mathbf{x}_0}{\int_{\text{cell}} |\Phi_m(\mathbf{x}_0)|^2|\Phi_n(\mathbf{x}_0)|^2 n(\mathbf{x}_0)d\mathbf{x}_0}. \quad (2.32)$$

From these definitions, it is clear that the redistribution and enhancement of the field energy in the Bloch modes of both the pump laser field and Stokes field and their simultaneous overlap with the distribution of Raman-active atoms in photonic crystals may lead to a strong enhancement of the Raman gain and of the atomic nonlinear response. Also, near a photonic band edge, the cavity-leakage rate γ_m is proportional to $|\hat{\mathbf{q}}\cdot\mathbf{v}_m|$ (where $\hat{\mathbf{q}}$ is the propagation direction) [26] and may be dramatically reduced due to the decrease of the group velocity in this frequency region [6]. We note that Eqs. (2.26)–(2.28) reduce to the semiclassical equations for stimulated Raman scattering in a homogeneous material when the dielectric function is constant and the carrier waves $\{\Phi_m(\mathbf{x})\}_m$ are plane waves.

III. CHARACTERISTICS OF STIMULATED RAMAN SCATTERING IN PHOTONIC CRYSTALS

In this section we apply the formalism developed in Sec. II to investigate the effect of the photonic crystal on the SRS

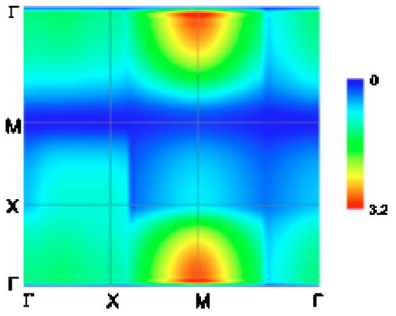

FIG. 4. (Color online) The scaled effective gain parameter $\bar{\alpha}_{mn}$ for the pump mode sampling the TM modes in the fourth band (horizontal axis) and the Stokes mode in the first band (vertical axis). The photonic crystal parameters are the same as for Fig. 2.

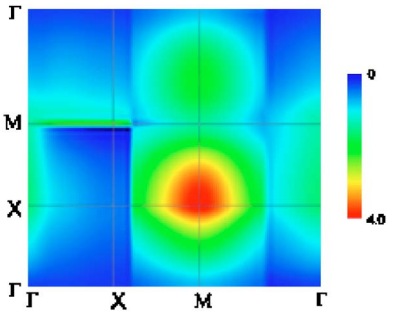

FIG. 5. (Color online) The same as for Fig. 4, but with the Stokes mode in the second band.

threshold and Raman signal, and present a possible practical realization of SRS in photonic crystals.

A. SRS threshold and efficiency

We will now discuss the effect of the photonic crystal on the threshold and the efficiency of stimulated Raman amplification. This discussion is facilitated by the presence in the effective semiclassical SRS Eqs. (2.26)–(2.28) of the photonic-crystal related effective parameters $\mathbf{v}_m$, α_{mn}, and β_{mn}. We consider a steady-state regime and set the time-derivatives in Eqs. (2.26)–(2.28) equal to zero. In this case, the steady-state nonlinear polarization $\mathcal{P}(\mathbf{x},t)$ can be expressed as

$$\mathcal{P}(\mathbf{x}) = i\frac{\kappa}{\gamma}\frac{\mathcal{N}}{1+4\beta_{nm}\dfrac{|\tilde{\Omega}_s(\mathbf{x})|^2|\tilde{\Omega}_L(\mathbf{x})|^2}{\Delta^2\Gamma\gamma}}\mathcal{E}_s(\mathbf{x})\mathcal{E}_L^*(\mathbf{x}). \quad (3.1)$$

Here we have defined the Stokes and pump Rabi frequencies $\tilde{\Omega}_s \equiv d_{32}\mathcal{E}_s/\hbar$ and $\tilde{\Omega}_L \equiv d_{31}\mathcal{E}_L/\hbar$. Substituting this expression into the propagation Eq. (2.26) for the Stokes field envelope function, we arrive at the propagation equation for the Stokes field intensity $I_s(\mathbf{x}) \equiv |\mathcal{E}_s(\mathbf{x})|^2$:

$$\mathbf{v}_m \cdot \nabla I_s(\mathbf{x}) = [-2\gamma_m + \mathcal{G}_{mn}I_L(\mathbf{x})]I_s(\mathbf{x}). \quad (3.2)$$

Here

$$\mathcal{G}_{mn} \equiv \frac{4\pi\kappa^2\omega_m}{\gamma}\frac{\mathcal{N}}{1+4\beta_{nm}\dfrac{|\tilde{\Omega}_s(\mathbf{x})|^2|\tilde{\Omega}_L(\mathbf{x})|^2}{\Delta^2\Gamma\gamma}}\alpha_{mn} \quad (3.3)$$

is the nonlinear gain coefficient for SRS in photonic crystals. We notice that it depends on both the effective gain and nonlinear coupling parameters, α_{mn} and β_{mn}, and an enhancement of α_{mn} will directly lead to enhanced Raman gain. Similarly, the equation for the pump modes propagating in the photonic crystal may be generally written as

$$\mathbf{v}_n \cdot \nabla I_L(\mathbf{x}) = \left[-2\gamma_n - \frac{\omega_n}{\omega_m}\mathcal{G}_{mn}I_s(\mathbf{x})\right]I_L(\mathbf{x}). \quad (3.4)$$

Here the intensity of the pump field is defined as $I_L(\mathbf{x}) \equiv |\mathcal{E}_L(\mathbf{x})|^2$, and the decay rate γ_n is associated with material losses (absorption of the pump laser field by nonresonant atoms).

In order to determine the threshold pump intensity necessary for amplification of the Stokes field, we assume that there is no nonlinear depletion of the pump field [described by the second term within the brackets on the right-hand side of Eq. (3.4)]. This assumption is justified for the values of the optical fields used in most of the experimental situations [27]. Further, we consider that the material losses are negligible for the frequency range of interest. Thus, within a leading approximation, the pump intensity is assumed to be nearly constant throughout the photonic crystal sample: $I_L(\mathbf{x}) \approx I_{Lo}$, where I_{Lo} is the incident pump intensity.

For small values of the Stokes and pump fields (below saturation regime) such that $\gamma\Delta, \Gamma\Delta \gg |\tilde{\Omega}_L|^2 \gg |\tilde{\Omega}_s|^2$, the term $4\beta_{nm}|\Omega_s(\mathbf{x})|^2|\Omega_L(\mathbf{x})|^2/\Delta^2\Gamma\gamma$ in the expression (3.3) of the gain coefficient can be neglected. From propagation Eq. (3.2) it follows that in this case the Stokes field envelope grows exponentially within the sample if

$$\mathcal{G}_{mn}^{(0)}I_{Lo} \geq 2\gamma_m, \quad (3.5)$$

where

$$\mathcal{G}_{mn}^{(0)} \equiv \frac{4\pi\kappa^2\omega_m\mathcal{N}}{\gamma}\alpha_{mn} \quad (3.6)$$

is the unsaturated SRS gain coefficient. Condition (3.5) represents the definition of the threshold for stimulated Raman scattering in photonic crystals. From Eqs. (3.5) and (3.6), the threshold intensity I_{thr} for SRS in photonic crystals can be expressed as

$$I_{thr} = \frac{\bar{\gamma}_m}{\bar{\alpha}_{mn}}I_o. \quad (3.7)$$

Here $I_o \equiv (\gamma/2\pi\kappa^2\omega_m\mathcal{N})(\gamma_o/\alpha_0)$ is the SRS threshold pump intensity in a uniform material (free space), and $\bar{\gamma}_m \equiv \gamma_m/\gamma_0$ and $\bar{\alpha}_{mn} \equiv \alpha_{mn}/\alpha_0$ are the loss and gain parameters, scalded to their free-space values, γ_0 and α_0, respectively. $\bar{\alpha}_{mn} > 1$ will express SRS gain enhancement in photonic crystals relative to free space.

The effect of the photonic crystal on the threshold pump intensity for stimulated Raman scattering is now evident from Eq. (3.7). We can see that redistribution and enhancement of the field energy of both pump and Stokes modes in

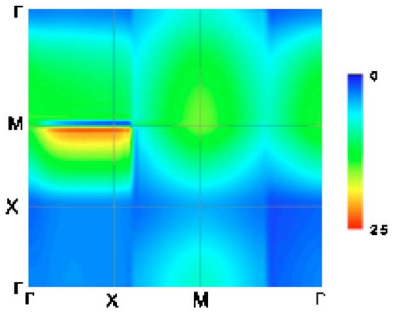

FIG. 6. (Color online) The same as for Fig. 4, but with the Stokes mode in the third band.

photonic crystals, leading to gain enhancement, together with alterations in the group velocity of the electromagnetic modes near a photonic band edge, leading to a dramatic decrease of the cavity decay rate γ_m, may result in a substantial decrease of the SRS pump threshold in photonic crystals.

We now analyze the generated Stokes field, and, for simplicity, consider the saturation regime. For sufficiently large values of the pump and Stokes fields, the exponential spatial growth of the Stokes field saturates. The saturation regime corresponds to setting the spatial derivatives in propagation Eq. (3.2) equal to zero. Using the definition (3.3) of the nonlinear gain coefficient $\mathcal{G}_{mn}$, we can express the saturation value of the Stokes field intensity, $\bar{I}_{sat}$, as

$$\bar{I}_{sat} = \frac{\gamma\Gamma}{4\kappa^2\beta_{nm}I_L}\left(\frac{I_L}{I_{thr}} - 1\right). \tag{3.8}$$

For a system operating well above threshold, $I_L/I_{thr} \gg 1$, we obtain

$$\bar{I}_{sat} = \frac{1}{\bar{\gamma}_m}\frac{\bar{\alpha}_{mn}}{\bar{\beta}_{mn}}\bar{I}_{sat}^{(0)}. \tag{3.9}$$

Here, $\bar{I}_{sat}^{(0)} \equiv \gamma\Gamma/4\kappa^2\beta_0 I_0$ is the saturation value of the Stokes field intensity in free space, and $\bar{\beta}_{mn} \equiv \beta_{mn}/\beta_0$ is the scaled value of the nonlinear coupling parameter β_{mn} to its free space value β_0. Again, we obtain that small cavity decay rates, corresponding to small group velocities near a photonic band edge, together with an enhancement of the gain parameter relative to the nonlinear coupling parameter, may lead to an enhanced stimulated Raman signal in photonic crystals.

B. Practical realization of SRS in a photonic crystal

We now illustrate how the formalism developed above could be employed to identify the optimal conditions for stimulated Raman scattering in photonic crystals. As an example, we consider a two-dimensional photonic crystal, consisting of a square lattice of dielectric cylinders in air. The lowest energy bands of the TM band structure for such a photonic crystal are presented in Fig. 2, and the group velocity for these energy bands is presented in Fig. 3.

Consider now that the Raman active material is uniformly distributed in the air fraction of this photonic crystal. Figures 4–6 present the scaled effective gain parameter $\bar{\alpha}_{mn}$ for the case when the pump mode corresponds to the points in the band 4 (horizontal axis), and the Stokes mode varies to correspond to the points in the lowest three bands (vertical axis). We obtain the largest enhancement of the SRS gain for the case when the system is pumped near the M point in the fourth band and the Stokes mode corresponds to the X point

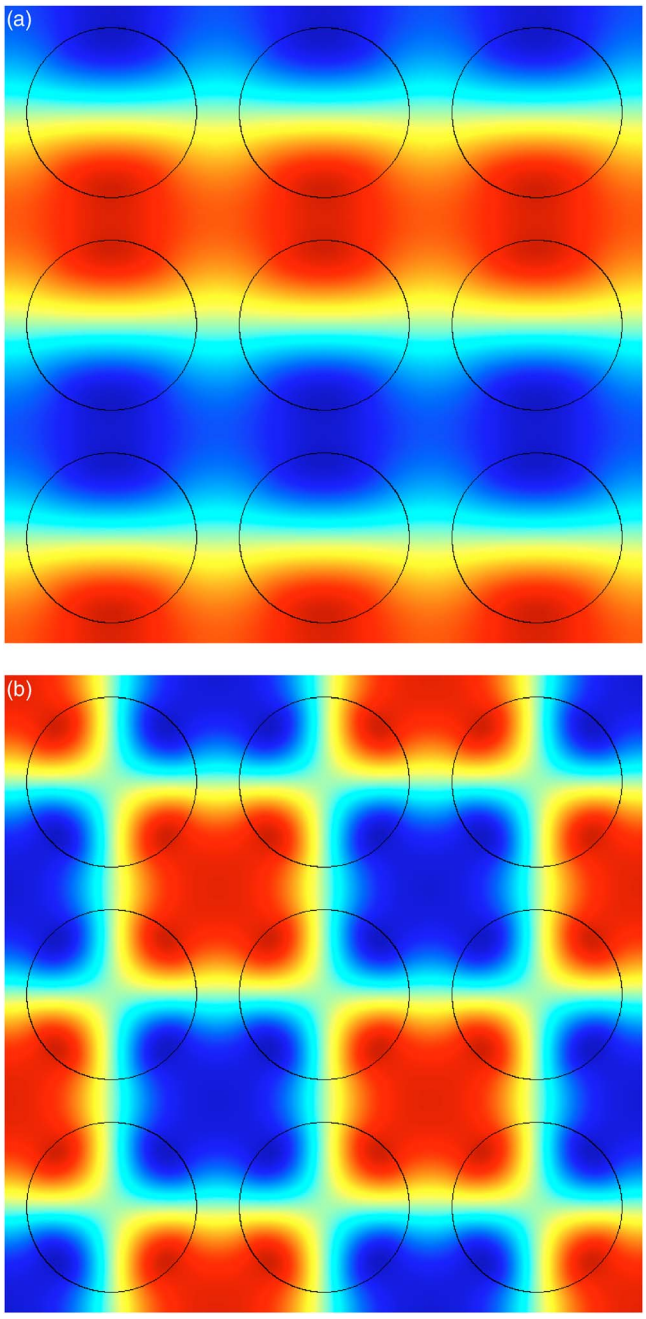

FIG. 7. (Color online) The electric field pattern of the TM modes inside a square array of dielectric cylinders in air. The dotted circles indicate the cylinders, and the color indicates the magnitude of the field. Dark blue and red regions are the regions where the field energy is concentrated. The mode at the X point in band 2 is shown on the left, and the mode at the M point in band 4 is shown on the right. The photonic crystal parameters are the same as for Fig. 2.

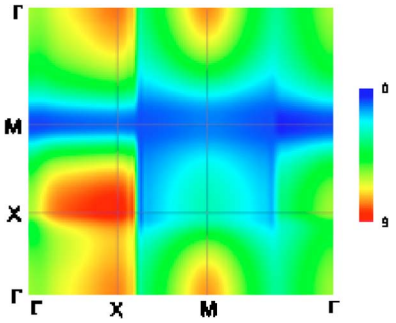

FIG. 8. (Color online) The scaled effective nonlinear coupling parameter $\bar{\beta}_{mn}$ for the same situation as for Fig. 4.

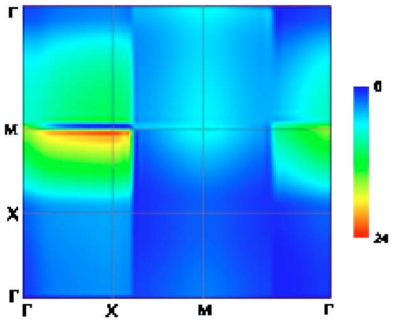

FIG. 10. (Color online) The scaled effective nonlinear coupling parameter $\bar{\beta}_{mn}$ for the same situation as for Fig. 6.

in the second band (Fig. 5). A (lower) gain enhancement can be also obtained when the pump is at point M in the fourth band and the Stokes mode is at point Γ in the first band (Fig. 4). However, as we can see from Fig. 3, the group velocity has a very low value only near the X point in the second band (as opposed to the Γ point in the first band, where it has a quite large value), thereby leading to very small decay rates for the Stokes field generated at this point. As a result, the lowest threshold for stimulated Raman scattering [Eq. (3.7)] is obtained when the pump mode corresponds to the M point in the fourth band and the stimulated Raman signal corresponds to point X in the second band. The gain enhancement in this case can be explained by the fact that the field energy of both the pump mode and Stokes mode is concentrated in the air fraction of the photonic crystal, where we assume the Raman active atoms are infiltrated. This can be seen in Fig. 7, where we present the electric field patterns for modes at the X point in the second band and at the M point in the fourth band.

Figures 8–10 present the scaled nonlinear coupling parameter $\bar{\beta}_{mn}$ for the same system and situations considered for Figs. 4–6, respectively. We obtain that the nonlinear coupling parameter has a similar behavior to that of the effective gain parameter. Although the gain and nonlinear coupling enhancement effects on the amplified Raman signal offset each other [see Eq. (3.9)], significant enhancement of the Stokes signal relative to that in free space is possible as a result of the dramatic lowering of the decay rate due to very small values of the group velocity at the photonic band edge (in this case, X point in the second band). This clearly demonstrates that both a low SRS threshold and enhanced Raman signal are possible near a photonic band edge in a photonic crystal.

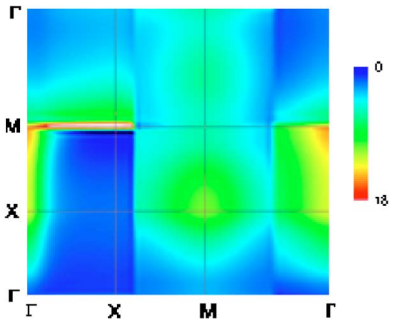

FIG. 9. (Color online) The scaled effective nonlinear coupling parameter $\bar{\beta}_{mn}$ for the same situation as for Fig. 5.

The existing capabilities to fabricate photonic crystals should enable the practical realization of SRS in these materials. Raman active material used for Stokes SRS experiments in photonic crystals have to be characterized by a vibrational transition frequency given by the frequency resonance condition (2.25). For a 2D photonic crystal such as that considered in the example above, the vibrational transition frequency is related to the lattice constant a of the photonic crystal through $\omega_{21} \approx 0.14(2\pi c/a)$. Thus, for a lattice constant of 200 nm, the corresponding vibrational frequency should be of the order of 2.1 THz (which corresponds to a vibrational transition wavelength of 0.35 μm). One Raman active material that has such vibrational transition characteristics is the Rhodamine 6G laser dye.

IV. CONCLUSION

We have investigated the stimulated Raman scattering by an atomic system embedded in a photonic crystal. Using a multiscale analysis, in which both the pump and Stokes pulses are approximated by an envelope function modulating a Bloch mode as a carrier wave, we have derived the semiclassical Maxwell-Bloch equations for the stimulated Raman scattering in photonic crystals. These equations are similar to those for stimulated Raman scattering in a uniform material, and contain effective parameters, calculated in terms of the Bloch modes of the linear, lossless photonic crystal. These parameters representing the group velocity, linear gain, and nonlinear coupling between the atomic system and the radiation field facilitate a direct investigation of the SRS characteristics in photonic crystals. We have shown that the spatial redistribution and enhancement of the field energy in the carrier modes in photonic crystals, together with small group velocities of the carrier waves near a photonic band edge, may lead to a dramatic lowering of the SRS threshold and to a strong enhancement of the Stokes field in photonic crystals.

In the present study we have investigated the stimulated Raman scattering at a photonic band edge in a pure photonic crystal, with no engineered defects. Another physical realization of stimulated Raman scattering in photonic crystals may employ an engineered localized defect mode acting as an

optical cavity. In this case, a strong enhancement of the Raman scattering process is expected as a result of the strong enhancement of the optical field near the localized mode.

It will be of considerable interest to extend the semiclassical model presented here to a fully quantized model of SRS in photonic crystals. A quantum theory is necessary to investigate the SRS spectrum, as well as the coherence properties of the scattered Stokes field. It will also allow for the investigation of Raman amplification in a microcavity embedded in a photonic crystal. Enhanced cavity field and better coherence have already been predicted for a one-atom laser in a photonic band-gap microchip [8].

ACKNOWLEDGMENTS

This work was supported by the National Science Foundation Nano-scale Science and Engineering Center (DMI-0327077) and California Nanosystem Institute (CNSI)/ Hewlett Packard Postdoctoral Fellowship Program.

[1] S. John, Phys. Rev. Lett. **53**, 2169 (1984).
[2] E. Yablonovitch, Phys. Rev. Lett. **58**, 2059 (1987).
[3] S. John, Phys. Rev. Lett. **58**, 2486 (1987).
[4] M. Meier, A. Mekis, A. Dodabalapur, A. Timko, R. E. Slusher, J. D. Joannopoulos, and O. Nalamasu, Appl. Phys. Lett. **74**, 7 (1999); M. Imada, S. Noda, A. Chutinan, T. Tokuda, M. Murata, and G. Sasaki, *ibid.* **75**, 316 (1999).
[5] O. Painter *et al.*, Science **284**, 1819 (1999).
[6] J. P. Dowling, M. Scalora, M. J. Bloemer, and C. M. Bowden, J. Appl. Phys. **75**, 1896 (1994).
[7] L. Florescu, K. Busch, and S. John, J. Opt. Soc. Am. B **19**, 2215 (2002).
[8] L. Florescu, S. John, T. Quang, and R. Wang, Phys. Rev. A **69**, 013816 (2004).
[9] S. John and T. Quang, Phys. Rev. Lett. **78**, 1888 (1997).
[10] M. Florescu and S. John, Phys. Rev. A **64**, 033801 (2001).
[11] M. Florescu and S. John, Phys. Rev. A **69**, 053810 (2004).
[12] *Surface Enhanced Raman Scattering*, edited by R. K. Chang and T. E. Furtak (Plenum Press, New York, 1982).
[13] M. Woldeyohannes, S. John, and V. I. Rupasov, Phys. Rev. A **63**, 013814 (2000).
[14] S. V. Gaponenko, Phys. Rev. B **65**, 140303(R) (2002).
[15] R. G. Zaporozhchenko, S. Ya Kilin, and A. G. Smirnov, Quantum Electron. **30**, 997 (2000).
[16] M. Scalora, M. J. Bloemer, A. S. Manka, J. P. Dowling, C. M. Bowden, R. Viswanathan, and J. W. Haus, Phys. Rev. A **56**, 3166 (1997).
[17] M. G. Raymer and J. Mostowski, Phys. Rev. A **24**, 1980 (1981).
[18] C. C. Gerry and J. H. Eberly, Phys. Rev. A **42**, 6805 (1990).
[19] H. J. Carmichael, *Statistical Methods in Quantum Optics 1* (Springer-Verlag, Berlin, 1999).
[20] A. Nayfeh, *Perturbation Methods* (Wiley, New York, 1973).
[21] C. M. de Sterke and J. E. Sipe, Phys. Rev. A **38**, 5149 (1988).
[22] N. A. R. Bhat and J. E. Sipe, Phys. Rev. E **64**, 056604 (2001).
[23] A. E. Siegman, *Lasers* (University Science Books, Sausalito, CA, 1986).
[24] J. E. Sipe, Phys. Rev. E **62**, 5672 (2000).
[25] D. Hermann, M. Frank, K. Busch, and P. Wölfle, Opt. Express **8**, 167 (2001).
[26] K. Sakoda, K. Ohtaka, and T. Ueta, Opt. Express **4**, 481 (1999).
[27] R. G. Smith, Appl. Opt. **11**, 2489 (1972).